Polarization properties of phase conjugation by degenerate four-wave mixing in a medium of rigidly held dye molecules

Wayne R. Tompkin, Michelle S. Malcuit, and Robert W. Boyd

Institute of Optics, University of Rochester, Rochester, New York 14627

John E. Sipe

Department of Physics, University of Toronto, Toronto, Ontario M5S 1A7, Canada

The saturation properties of dye molecules that are rigidly held in a solid host are qualitatively different from those of molecules that are free to rotate. We have found that these unique saturation characteristics can be exploited to achieve nearly perfect vector phase conjugation for field strengths near the saturation intensity. We have studied these properties experimentally by using fluorescein-doped boric acid glass as the nonlinear-optical material.

Organic dyes doped into solid matrices form an important and interesting class of optical materials. Indeed, some of the largest optical nonlinearities are those due to saturable absorption in organic molecules doped into various solids.[1,2] The nonlinear-optical properties of rigidly held molecules can differ substantially from the properties of isotropic absorbers such as atoms or of molecules that are free to rotate. For example, for a randomly oriented, rigidly held collection of anisotropically absorbing molecules, the rate at which the absorption saturates depends on the polarization state of the applied radiation, whereas the rate is independent of the polarization state for molecules that are free to rotate.[2,3] In this paper we demonstrate, through phase-conjugation experiments, that the polarization properties of degenerate four-wave mixing (DFWM) in fluorescein-doped boric acid glass are dramatically modified by this anisotropic saturation. In fact, we find that for linearly polarized pump waves and for a judicious choice of input intensities, DFWM in this material can lead directly to vector phase conjugation (VPC), that is, to simultaneous reversal of the optical wave front and conjugation of the state of polarization of the incident field.[4-8] Polarization conjugation would not occur for the case of linearly polarized pump waves for a Kerr-type [i.e., $\chi^{(3)}$] nonlinearity nor would it occur for a saturable absorber in which the molecules were free to rotate.

We model fluorescein-doped boric acid glass as a collection of rigidly held, randomly oriented dipoles. We assume that the dye molecule absorbs only the component of the incident field that is polarized along its chromophore.[9] It is convenient to express the molecular-transition dipole moment as $\mu = \mu\hat{\mu}$, where the unit vector $\hat{\mu}$ describes the orientation of the chromophore. The complex amplitude $\mathbf{P}$ of the polarization induced by an electric field of complex amplitude $\mathbf{E}$ acting on such a collection of uniformly and randomly oriented dipoles is given by[2]

$$\mathbf{P} = \frac{K}{|E_s|^2} \int d\Omega \frac{\hat{\mu}(\hat{\mu} \cdot \mathbf{E})}{1 + |\hat{\mu} \cdot \mathbf{E}|^2/|E_s|^2}, \qquad (1)$$

where $|E_s|^2$ is the saturation intensity for light polarized along the chromophore, $\int d\Omega$ denotes an orientational average over solid angle, and K is a proportionality constant that depends on the particular molecular system. In Eq. (1) we are using the convention that the fields are related to their complex amplitudes by $\mathbf{P}(r, t) = \mathbf{P} \exp(-i\omega t) + \text{c.c.}$ and $\mathbf{E}(r, t) = \mathbf{E} \exp(-i\omega t) + \text{c.c.}$ We assume that the dye molecule interacts with the applied field as a system of singlet and triplet states, which exchange population through intersystem crossing and delayed fluorescence,[9,10] as illustrated in Fig. 1. For this model the saturation intensity and proportionality constant K are given by $|E_s|^2 = \gamma\hbar^2(\Delta_1^2 + \Gamma_1^2)/4\Gamma_1|\mu|^2$ and $K = (N/4\pi)[\hbar\gamma(\Delta_1 + i\Gamma_1)/4\Gamma_1]$, where γ^{-1} is the ground-state recovery time, Δ_1 is the detuning of the applied field from the singlet–singlet transition, $(\Gamma_1)^{-1}$ is the dipole-relaxation time for the singlet–singlet transition, and N is the number density of molecules.

The nonlinear polarization $\mathbf{P}^{\text{NL}}$ is found by subtracting the linear contribution $(K/|E_s|^2)\int d\Omega\hat{\mu}(\hat{\mu} \cdot \mathbf{E})$ from the total polarization given by Eq. (1) to obtain

$$\mathbf{P}^{\text{NL}} = \frac{-K}{|E_s|^4} \int d\Omega \frac{\hat{\mu}(\hat{\mu} \cdot \mathbf{E})|\hat{\mu} \cdot \mathbf{E}|^2}{1 + |\hat{\mu} \cdot \mathbf{E}|^2/|E_s|^2}. \qquad (2)$$

We use DFWM to investigate the tensor properties of the nonlinear interaction. We take the total incident electric field $\mathbf{E}$ to be the sum of a strong pump field $\mathbf{E}_0$ and a weak probe field $\mathbf{E}_p$. The nonlinear polarization driving the conjugate wave is found by expanding the nonlinear polarization about the amplitude $\mathbf{E}_0$ of the strong pump field and keeping terms linear in $\mathbf{E}_p{}^*$:

$$\mathbf{P}_c = \frac{-K}{|E_s|^4} \int d\Omega \frac{\hat{\mu}(\hat{\mu} \cdot \mathbf{E}_0)^2(\hat{\mu} \cdot E_p{}^*)}{(1 + |\hat{\mu} \cdot \mathbf{E}_0|^2/|E_s|^2)^2}. \qquad (3)$$

Because we are interested in the vector nature of phase conjugation by DFWM, we find it useful to introduce a basis set of polarization unit vectors, which explicitly separates
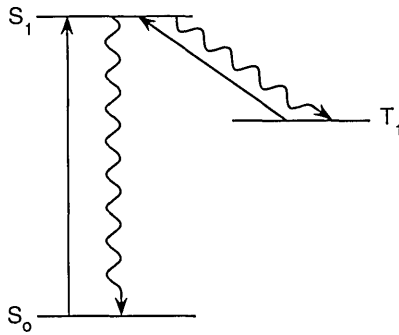
Fig. 1. Energy-level diagram showing the relevant optical interactions in fluorescein-doped boric acid glass. Following optical excitation from the singlet ground state S_0 to the singlet excited state S_1, population makes an intersystem crossing into the lowest-lying triplet state T_1. Because of its long luminescent lifetime ($\sim$0.1 sec), the lowest-lying triplet state T_1 acts as a trap level. At room temperature the principal relaxation route out of the triplet state is thermally activated delayed fluorescence, that is, a thermally excited transition from T_1 to S_1 followed by fluorescent decay back to the ground state.

out the polarization-conjugating and non-polarization-conjugating contributions to $\mathbf{P}_c$. We define $\hat{\epsilon}_g$ to be a unit vector that points in the direction of the complex conjugate of the polarization of the probe beam (i.e., $\hat{\epsilon}_g = \mathbf{E}_p{}^*/|\mathbf{E}_p|$) and $\hat{\epsilon}_b$ to be a vector that is orthogonal to $\hat{\epsilon}_g$, that is, $\hat{\epsilon}_b \cdot \hat{\epsilon}_g{}^* = 0$. The nonlinear polarization can be represented in this basis as

$$\mathbf{P}_c = P_g \hat{\epsilon}_g + P_b \hat{\epsilon}_b, \tag{4a}$$

where

$$P_{g,b} = \frac{-K}{|E_s|^4} \int d\Omega \, \frac{(\hat{\mu} \cdot \hat{\epsilon}_{g,b}{}^*)(\hat{\mu} \cdot \mathbf{E}_0)^2(\hat{\mu} \cdot \mathbf{E}_p{}^*)}{(1 + |\hat{\mu} \cdot \mathbf{E}_0|^2/|E_s|^2)^2}. \tag{4b}$$

Note that P_g is that part of the nonlinear polarization that leads to polarization conjugation (i.e., the "good" part of $\mathbf{P}_c$), whereas P_b (the "bad" part) leads to the generation of the incorrect polarization component.

Figure 2 shows the experimental setup that we used to investigate the tensor properties of the nonlinear interaction. The forward- and backward-traveling pump waves have equal field amplitudes A_0 (which for simplicity we take to be real), are polarized in the $\hat{x}$ direction, and propagate along the z' axis so that $\mathbf{E}_0 = 2A_0 \cos(kz')\hat{x}$, where k is the magnitude of the wave vector. The probe wave $\mathbf{E}_p$ propagates along the z axis and is represented as $\mathbf{E}_p = \mathbf{A}_p \exp(ikz) = A_p \exp(ikz)\hat{\epsilon}_g{}^*$. We assume that the angle between the z and z' axes is small. The experiment entails determining the polarization state of the generated conjugate beam. For this choice of linear pump wave polarizations, we can perform the orientational average of Eq. (3) analytically. To do so, we express $\hat{\mu}$ in the laboratory coordinate system $(\hat{x}, \hat{y}, \hat{z})$ as

$$\hat{\mu} = \hat{z} \sin\theta \cos\phi + \hat{y} \sin\theta \sin\phi + \hat{x} \cos\theta \tag{5}$$

and the solid angle element as $d\Omega = \sin\theta \, d\theta \, d\phi$. Note that we are using the somewhat unconventional polar coordinates θ and ϕ in order to allow us to use the pump polarization direction $\hat{x}$ as the polar axis. We find that

$$\mathbf{P}_c = P_x \hat{x} + P_y \hat{y}, \tag{6a}$$

where the Cartesian components of $\mathbf{P}_c$ are given by

$$P_x(z') = \frac{-\pi K A_{px}{}^* e^{-ikz}}{|E_s|^2} \left\{ \frac{2}{\alpha^2} \left[\frac{2\alpha^2 + 3}{\alpha^2 + 1} - \frac{3}{\alpha} \tan^{-1}(\alpha) \right] \right\} \tag{6b}$$

and

$$P_y(z') = \frac{-\pi K A_{py}{}^* e^{-ikz}}{|E_s|^2} \left\{ \frac{1}{\alpha^2} \left[\frac{3 + \alpha^2}{\alpha} \tan^{-1}(\alpha) - 3 \right] \right\}, \tag{6c}$$

where $\alpha = 2A_0 \cos(kz')/|E_s|$, where $\mathbf{A}_p{}^* = A_p{}^* \hat{\epsilon}_g = A_{px}{}^* \hat{x} + A_{py}{}^* \hat{y}$. The polarization-conjugating and orthogonal components of $\mathbf{P}_c$ can be obtained by equating Eqs. (4a) and (6a) to obtain

$$P_{g,b}(z') = P_x(z')(\hat{x} \cdot \hat{\epsilon}_{g,b}{}^*) + P_y(z')(\hat{y} \cdot \hat{\epsilon}_{g,b}{}^*). \tag{7}$$

We assume, for simplicity, that the medium is sufficiently thin that the pump and probe waves are of constant amplitude. The conjugate field $\mathbf{E}_c = \mathbf{C} \exp(-ikz)$ generated by the four-wave mixing process is found by solving the driven, reduced wave equation, which can be written as

$$d\mathbf{C}/dz = 2\pi i k \mathbf{P}_c{}^{\mathrm{pm}}. \tag{8}$$

where $\mathbf{P}_c{}^{\mathrm{pm}}$ is the phase-matched contribution to $\mathbf{P}_c$. The amplitude $\mathbf{P}_c$ contains a rapid spatial dependence due to the interference between the pump waves. We hence extract the phase-matched contributions to $\mathbf{P}_c$ by performing the spatial average

$$\mathbf{P}_c{}^{\mathrm{pm}} = (1/\lambda) \int_0^\lambda \exp(ikz)\mathbf{P}_c(z')dz'. \tag{9}$$

We have been unable to perform this average analytically and hence calculate $\mathbf{P}_c{}^{\mathrm{pm}}$ by numerical integration, using the simplifying assumption that $z = z'$. We represent the conjugate field $\mathbf{C}$ and nonlinear polarization $\mathbf{P}_c{}^{\mathrm{pm}}$ in terms of their good and bad components as $\mathbf{C}(z) = C_g(z)\hat{\epsilon}_g + C_b(z)\hat{\epsilon}_b$ and
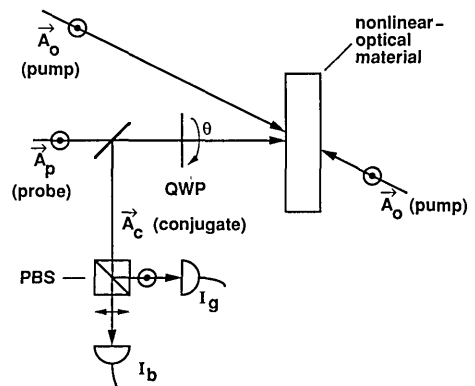
Fig. 2. Experimental setup used to study the polarization properties of DFWM. The quarter-wave plate (QWP) can be oriented at an arbitrary angle θ. For the experiments shown in Figs. 3 and 4, the fast axis of the quarter-wave plate is oriented at 45° to the input polarization direction so that the probe wave incident upon the nonlinear-optical medium is circularly polarized. If the DFWM process leads to perfect VPC, the effect of the quarter-wave plate will be removed in double pass, leading to a conjugate wave polarized in the initial polarization direction. Through the use of a polarizing beam splitter (PBS) and detectors, we measure the intensity I_g of the VPC (good) component and the intensity I_b of the orthogonal (bad) component.

$\mathbf{P}_c{}^{\mathrm{pm}} = P_g{}^{\mathrm{pm}}\hat{\epsilon}_g + P_b{}^{\mathrm{pm}}\hat{\epsilon}_b$. We can then express Eq. (8) as two scalar equations:

$$\frac{dC_g}{dz} = i\kappa_g{}^* A_p{}^*, \qquad \frac{dC_b}{dz} = i\kappa_b{}^* A_p{}^*, \qquad (10)$$

where the coupling constants $\kappa_g{}^*$ and $\kappa_b{}^*$ are given by

$$\kappa_g{}^* = 2\pi k(P_g{}^{\mathrm{pm}}/A_p{}^*), \qquad \kappa_b{}^* = 2\pi k(P_b{}^{\mathrm{pm}}/A_p{}^*). \qquad (11)$$

The components of the conjugate field at the output of the interaction region of length l are then given by the solutions of Eq. (10), with the boundary condition $\mathbf{C}(l) = 0$ as

$$C_g(0) = -i\kappa_g{}^* l A_p{}^*, \qquad C_b(0) = -i\kappa_b{}^* l A_p{}^*. \qquad (12)$$

The intensities associated with these components are given by $I_g = |C_g(0)|^2$ and $I_b = |C_b(0)|^2$. Perfect VPC occurs if $I_b(0) = 0$ for $I_g(0) \neq 0$.

The predictions of the theory developed above are shown in Fig. 3(a). We assume that the probe beam is right-hand circular polarized. Then its polarization unit vector is $\hat{\epsilon} = (\hat{x} - i\hat{y})/\sqrt{2}$, and consequently $\hat{\epsilon}_g = \hat{\epsilon}^* = (\hat{x} + i\hat{y})/\sqrt{2}$ and $\hat{\epsilon}_b = (\hat{x} - i\hat{y})/\sqrt{2}$. Because the conjugate wave propagates in the negative z direction, $\hat{\epsilon}_g$ and $\hat{\epsilon}_b$ correspond to right- and left-hand circular polarization, respectively. Note that an ideal VPC mirror produces only the $\hat{\epsilon}_g$ component and hence preserves the handedness of a beam of light on reflection instead of inverting it, as is the case for an ordinary mirror. In Fig. 3(a) we plot the phase-conjugate reflectivities $R_{g,b} = I_{g,b}/|A_p|^2$ associated with the right-hand (good) and left-hand circular (bad) polarization components as functions of the total input intensity $I = 2A_0^2$. We see that R_g is everywhere greater than R_b and that for a particular value of I/I_{sat} (~ 3) the intensity of the bad component vanishes, implying that in this case perfect VPC occurs. This result can be understood conceptually by studying the rate at which the terms in curly braces in Eqs. (6b) and (6c) saturate as A_0^2 is increased. At low pump intensities the molecular response is larger for probe fields polarized parallel to the pump polarization ($\hat{x}$) direction than for probe fields polarized in the perpendicular ($\hat{y}$) direction. However, at high pump intensities the response in the direction of the pump polarization is nearly completely saturated, and hence the response for the $\hat{y}$ component of the probe is greater than that for the $\hat{x}$ component. At some intermediate intensity the response of the two components is equal, and perfect VPC is predicted in this case.

To test these theoretical predictions, we performed the experiment shown in Fig. 2, using fluorescein-doped boric acid glass as the nonlinear-optical material. We chose fluorescein-doped boric acid glass because it has a low saturation intensity and because thin samples of high optical quality are easily fabricated.[2] The sample used in this experiment had an effective response time of ~ 100 msec, a small-signal absorption $\alpha_0 l = 0.6$ at 457.9 nm, a saturation intensity of ~ 100 mW/cm^2, and a thickness of ~ 100 μm. An argon-ion laser was used to produce two beams of equal intensity and of parallel linear polarization, which formed the counterpropagating pump beams. We used a probe beam having an intensity equal to 5% of that of one of the pump beams.

In our experiment the probe beam is initially linearly polarized parallel to the direction of polarization of the pump beams. The probe beam then passes through a quarter-wave plate oriented with its fast axis at an angle of 45°
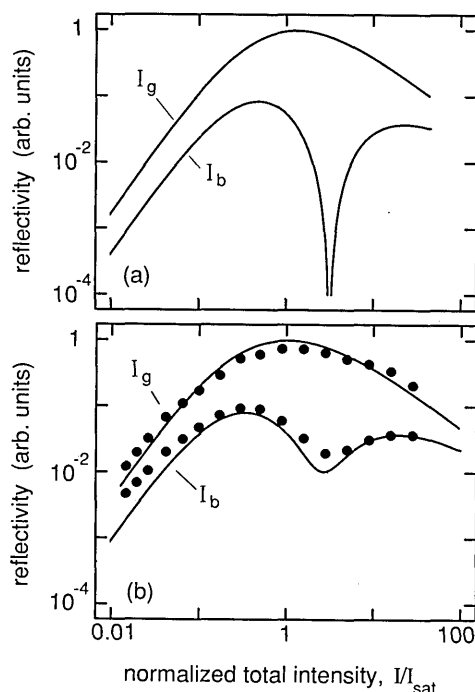
Fig. 3. Reflectivity associated with each polarization component plotted as a function of normalized pump intensity I/I_{sat}. The solid curves in (a) were calculated by assuming a single saturation intensity, and the solid curves in (b) were calculated assuming a 40%-wide Gaussian distribution of saturation intensities. The circles represent experimental data and are plotted using the value $I_{\mathrm{sat}} = 100$ mW/cm^2. Note that the reflectivity of the good component is greater than that of the bad component and becomes much greater than R_b for intensities near the saturation intensity.

with respect to the input-beam polarization direction, as shown in Fig. 2, and is thus rendered circularly polarized when incident upon the nonlinear-optical medium. The experiment entails determining the extent to which the VPC process is capable of removing the effects of the quarter-wave plate on double pass. A polarization-insensitive beam splitter samples the conjugate beam, and a prism polarizer analyzes the state of polarization of the beam. The intensity components of the conjugate beam parallel to (I_g) and orthogonal to (I_b) the original polarization direction are measured.

The circles in Fig. 3(b) show the measured values of the reflectivities R_g and R_b. We find, as theory predicts, that R_g is always greater than R_b and becomes much greater than R_b for pump intensities somewhat above the saturation intensity. However, the minimum value of R_b never drops to zero. We believe that this disagreement results from the fact that there is a distribution of saturation intensities in the fluorescein-doped boric acid glass. It was shown previously that site-to-site variations in the local fields that the molecules experience[10,11] cause a spread in the decay times and, hence, in the saturation intensities.[9,12,13] The solid curves in Fig. 3(b) show the predictions of the theory under the assumption that there is a spread of saturation intensities. These curves are obtained by convolving the results of Fig. 3(a) with a Gaussian distribution of saturation intensities with a standard deviation that is 40% of the mean. We see that these predictions are in good agreement with the results of the experiment.
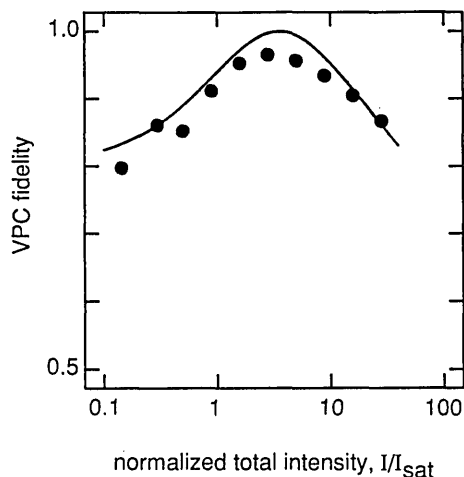
Fig. 4. Fidelity of the VPC process versus the normalized pump intensity. VPC fidelity is defined as the ratio $I_g/(I_g + I_b)$, that is, as the ratio of the intensity of the proper polarization component to the total output intensity. The circles represent experimental data plotted using $I_{sat} = 100$ mW/cm^2, and the solid curve is calculated using the theory described in the text.
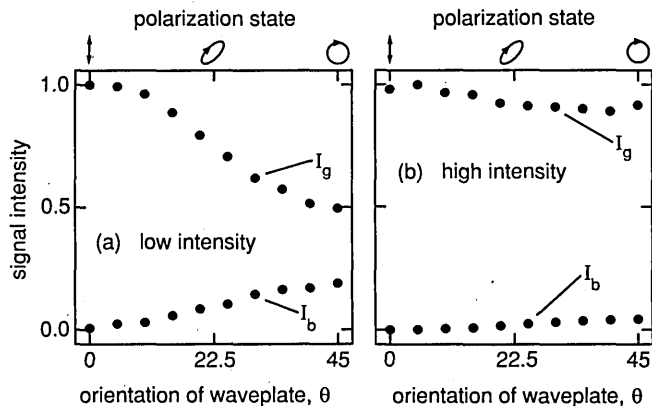
Fig. 5. Intensity of each polarization component (in arbitrary units) plotted as a function of the state of polarization of the probe wave after it passes through the quarter-wave plate. (a) For low pump intensities ($0.01I_{sat}$), severe degradation of the polarization properties of the phase-conjugation process is observed (I_g and I_b are comparable and show a strong dependence on θ). (b) For pump intensities near the saturation intensity ($2I_{sat}$), the effects of the polarization distortion are largely removed ($I_b \ll I_g$ and I_g is independent of θ).

Figure 4 shows more quantitatively how the vector nature of the DFWM process varies with pump intensity. We take the quantity $I_g/(I_g + I_b)$ to be a measure of the fidelity of the VPC process.[7] The data points are seen to be in good agreement with the theory, again assuming a 40%-wide distribution of saturation intensities. For pump intensities near the saturation intensity, the fidelity is seen to be nearly perfect. We believe that the fidelity of the VPC process would be even closer to unity if there were no site-to-site variations in the local environment experienced by individual molecules or if the dye molecules were insensitive to these small variations.

We also studied how the tensor properties of phase conju-

gation depend on the state of polarization of the probe beam. We vary the polarization of the probe beam by changing the rotation angle θ of the quarter-wave plate shown in Fig. 2. We then measure the extent to which the effects of the polarization distortion are removed after the conjugate beam passes through the quarter-wave plate. The experimental results shown in Fig. 5 demonstrate that for pump intensities near the saturation intensity the effects of the polarization distortion are essentially removed, whereas at low pump intensities [i.e., in the $\chi^{(3)}$ limit] the system is unable to compensate for the polarization distortion on double pass.

In conclusion, we have shown that DFWM using a dye-doped solid host can lead to nearly perfect VPC when pumped by linearly polarized pump waves with intensities slightly above the saturation intensity.

ACKNOWLEDGMENTS

REFERENCES

1. T. A. Shankoff, Appl. Opt. 8, 2282 (1969); Y. Silberberg and I. Bar-Joseph, Opt. Commun. 39, 265 (1981); I. Bar-Joseph and Y. Silberberg, Opt. Commun. 41, 455 (1982); M. A. Kramer, W. R. Tompkin, and R. W. Boyd, J. Lumin. 31/32, 789 (1984); H. Fugiwara and K. Nakagawa, Opt. Commun. 55, 386 (1985); T. Todorov, L. Nikolova, N. Tomova, and V. Dragostina, Opt. Quantum Electron. 13, 209 (1981); IEEE J. Quantum Electron. QE-22, 1262 (1986); W. R. Tompkin, R. W. Boyd, D. W. Hall, and P. A. Tick, J. Opt. Soc. Am. B. 4, 1030 (1987).
2. M. A. Kramer, W. R. Tompkin, and R. W. Boyd, Phys. Rev. A 34, 2026 (1986).
3. M. Montecchi, M. Settembre, and M. Romagnoli, J. Opt. Soc. Am. B 5, 2357 (1988).
4. N. G. Basov, V. F. Efimkov, I. G. Zuberev, A. V. Kotov, S. I. Mikhailov, and M. G. Smirnov, JETP Lett. 28, 197 (1978); I. McMichael, M. Khoshnevisan, and P. Yeh, Opt. Lett. 11, 525 (1986); K. Kyuma, A. Yariv, and S.-K. Kwong, Appl. Phys. Lett. 49, 617 (1986); I. McMichael, P. Yeh, and P. Beckwith, Opt. Lett. 12, 507 (1987); I. McMichael, J. Opt. Soc. Am. B 5, 863 (1988).
5. V. N. Blaschuk, B. Ya. Zel'dovich, A. V. Mamaev, N. F. Pilipetsky, and V. V. Shkunov, Sov. J. Quantum Electron. 10, 356 (1980); G. Martin, L. L. Lam, and R. W. Hellwarth, Opt. Lett. 5, 185 (1980).
6. G. Grynberg, Opt. Commun. 48, 432 (1984); M. Ducloy and D. Bloch, Phys. Rev. A 30, 3107 (1984); S. Saikan and M. Kiguchi, Opt. Lett. 7, 555 (1982).
7. M. S. Malcuit, D. G. Gauthier, and R. W. Boyd, Opt. Lett. 13, 663 (1988).
8. L. L. Chase, M. L. Claude, D. Hulin, and A. Mysryrowicz, Phys. Rev. A 28, 3969 (1983).
9. G. N. Lewis, D. Lipkin, and T. T. Magel, J. Am. Chem. Soc. 63, 3005 (1941).
10. M. Frakowiak and H. Waylerys, Acta Phys. Polon. 18, 93 (1959).
11. T. Tomashek, Ann. Phys. 67, 622 (1922).
12. D. W. Greggs and H. G. Drickamer, J. Chem. Phys. 35, 1780 (1960).
13. V. A. Pilipovitch and B. T. Sveshnikov, Opt. Spektrosk. 5, 290 (1958).